Published in final edited form as:
Osteoarthritis Cartilage. 2021 May 01; 29(5): 762–772. doi:10.1016/j.joca.2021.01.009.

Quantitative three-dimensional collagen orientation analysis of human meniscus posterior horn in health and osteoarthritis using micro-computed tomography

V-P. Karjalainen[1], **I. Kestilä**[1], **M.A. Finnilä**[1,2], **E. Folkesson**[3,4], **A. Turkiewicz**[3], **P. Önnerfjord**[4], **V. Hughes**[3], **J. Tjörnstrand**[5], **M. Englund**[3,*], **S. Saarakkala**[1,6,*]

[1]Research Unit of Medical Imaging, Physics and Technology, Faculty of Medicine, University of Oulu, Oulu, Finland [2]Medical Research Center, University of Oulu, Oulu, Finland [3]Lund University, Faculty of Medicine, Department of Clinical Sciences Lund, Orthopaedics, Clinical Epidemiology Unit, Lund, Sweden [4]Lund University, Faculty of Medicine, Department of Clinical Sciences Lund, Rheumatology and Molecular Skeletal Biology, Lund, Sweden [5]Lund University, Skåne University Hospital, Department of Clinical Sciences Lund, Orthopaedics, Lund, Sweden [6]Department of Diagnostic Radiology, Oulu University Hospital, Oulu, Finland

Abstract

Objective—Knee osteoarthritis (OA) is associated with meniscal degeneration that may involve disorganization of the meniscal collagen fiber network. Our aims were to quantitatively analyze the microstructural organization of human meniscus samples in 3D using micro-computed tomography (μCT), and to compare the local microstructural organization between OA and donor samples.

Method—We collected posterior horns of both medial and lateral human menisci from 10 end-stage medial compartment knee OA patients undergoing total knee replacement (medial & lateral OA) and 10 deceased donors without knee OA (medial & lateral donor). Posterior horns were

[*]Equal contribution as senior authors

Author contributions

Conception and design: VPK, IK, MF, ME and SS
Provision of study materials and tissue preparation: ME, EF, VH, PÖ, JT, IK and MF, SS
Micro-CT imaging: IK and MF
Image processing/assessment: VPK and IK
Statistical analysis: VPK and AT
Interpretation of results: All coauthors
Drafting of the article: VPK
Critical revision of the article for important intellectual content: IK, MF, EF, AT, PÖ, VH, JT, ME and SS.
Final approval of the article: All coauthors

Conflict of interest

AT works as an associate editor (statistics) in Osteoarthritis and Cartilage.
ME has received grants from European Research Council, The Swedish Research Council, the Foundation for Research in Rheumatology, the Greta and Johan Kock Foundation, the Swedish Rheumatism Association, the Österlund Foundation, the Governmental Funding of Clinical Research program within the National Health Service in Sweden, and the Faculty of Medicine, Lund University, Sweden.
ME reports in 2019 serving on an advisory board for Pfizer (Tanezumab).
SS has received grants from Foundation for Research in Rheumatology and European Research Council.
Other authors (VK, IK, MF, EF, PÖ, VH, and JT) report no conflicts of interest.

Europe PMC Funders Author Manuscripts

dissected and fixed in formalin, dehydrated in ascending ethanol concentrations, treated with hexamethyldisilazane (HMDS), and imaged with μCT. We performed local orientation analysis of collagenous microstructure in 3D by calculating structure tensors from greyscale gradients within selected integration window to determine the polar angle for each voxel.

Results—In donor samples, meniscus bundles were aligned circumferentially around the inner border of meniscus. In medial OA menisci, the organized structure of collagen network was lost, and main orientation was shifted away from the circumferential alignment. Quantitatively, medial OA menisci had the lowest mean orientation angle compared to all groups, -24° (95%CI -31 to -18) vs medial donor and -25° (95%CI -34 to -15) vs lateral OA.

Conclusions—HMDS-based μCT imaging enabled quantitative analysis of meniscal collagen fiber bundles and their orientations in 3D. In human medial OA menisci, the collagen disorganization was profound with overall lower orientation angles, suggesting collagenous microstructure disorganization as an important part of meniscus degradation.

Keywords

osteoarthritis; collagen organization; meniscus microstructure; contrast agent free micro-computed tomography; structure tensors

Introduction

The human meniscus is a fibrocartilaginous soft tissue that has an important roles in knee joint function including load bearing, load transmission, joint lubrication, nutrition distribution, shock absorption, and the ability to withstand different mechanical forces such as compression, shear and tension[1–7]. The extracellular matrix (ECM) of a healthy meniscal body consists of a thick network of collagen fibers (20-25% of wet weight) working as a principal solid component of the ECM, together with other constituents, such as water (65-75% of wet weight), proteoglycans (<1% of wet weight) and non-collagenous proteins[8–10].

Cross-sectionally, the meniscus has three distinct layers with different collagen structures[11]. A superficial layer covers the femoral and tibial surfaces of the menisci with thin but dense randomly oriented collagen fiber network that is parallel to the surface[11,12]. The layer beneath is the lamellar layer with fibers oriented towards the femoral and tibial surfaces, forming arc-like structures intersecting with the superficial layer's fibers[6,11,12]. The middle layer of meniscus lies between the lamellar layers and is formed by collagen fiber bundles of varying sizes[11], with a single collagen fiber diameter ranging from 5 μm to 10 μm[13]. The collagen fibers in the middle layer orient circumferentially around the inner border of meniscus, and with the middle layer covering most of the tissue volume in meniscus, circumferential orientation is the predominant alignment of the collagen fibers in the whole meniscus[6,11,12,14]. In the outer border of both medial and lateral menisci, radial collagen bundles orient orthogonally and intertwine with circumferentially aligned fibers, tying the meniscus together[11,15,16]. These bundles provide additional mechanical reinforcement and prevent separation of circumferentially oriented bundles[17].

In knee osteoarthritis (OA), it has been reported that meniscal tears and degeneration are associated with disorganization of the collagen fiber network of the meniscus, and that the posterior horn of the medial meniscus is the most susceptible region to these changes[14,18,19]. Besides disorganization of the collagen fiber network, increased water and proteoglycan contents, as well as decreased collagen content has been reported in the degenerated meniscus[8,19,20].

We have previously visualized the microstructure of the posterior horn of the human meniscus *ex vivo* using a hexamethyldisilazane (HMDS) based sample drying technique together with micro-computed tomography (μCT)[21]. HMDS-based sample processing enables contrast-agent-free μCT imaging of soft tissues, such as meniscus[21] and articular cartilage (AC)[22], by dehydrating the sample and creating intrinsic contrast within the soft tissue. In our preliminary study, an HMDS-based sample processing protocol was applied to quantitatively determine the extracellular matrix orientation in AC[23]. However, the local orientation of the collagenous microstructure of human meniscus has not been quantitatively analyzed in 3D and compared between end-stage OA patients and healthy donors.

In this study, our objectives were to: 1) analyze the microstructural organization of *ex vivo* human meniscus samples in 3D using our previously implemented HMDS-based μCT imaging protocol, and 2) quantitatively compare the local microstructural organization of meniscus posterior horn between medial and lateral menisci of end-stage medial compartment knee OA patients and deceased donors without known knee OA (healthy donors). We hypothesize that there are differences in the local microstructural organization between medial OA menisci and medial donor menisci, and that the lateral OA menisci are more similar to lateral donor menisci.

Methods

Tissue sample preparation

The regional ethical review board at Lund University approved this study (Dnr 2015/39 and Dnr 2016/865). The same sample set was used as in our previous study in which the sample selection is explained in more detail[21]. Briefly, human meniscus samples from the knee tissue biobank MENIX at Skåne University Hospital were used for this study. We selected both the medial and lateral menisci from the right knee of 10 deceased adult donors. The donors had no known diagnosis of knee OA or rheumatoid arthritis. From the same biobank, we also retrieved both the medial and lateral menisci collected from 10 end-stage medial compartment knee OA patients (all medial samples had Outerbridge grade IV, while lateral samples had grade 0 or I) during total knee replacement (TKR) surgery. Both OA and donor groups include five men and five women. Hereafter, these medial and lateral sample groups from deceased donors and TKR patients are referred to as medial donor and lateral donor, and medial OA and lateral OA, respectively. All the menisci were frozen at -80°C within 2 hours of extraction. The samples were thawed in phosphate buffered saline (PBS), and the posterior horn was separated from the meniscus body with a scalpel followed by fixation in 4% saline-buffered formaldehyde for a minimum of 11 days. A few millimeter-thick tissue sections were cut from the fixed posterior horns for μCT imaging and following analyses.

HMDS-based μCT imaging

The same μCT dataset was used as in our previous work[21]. Briefly, the fixed samples were dehydrated in ascending ethanol concentrations before treating them with HMDS and further leaving them to air-dry in a fume hood at room temperature overnight. For μCT image acquisition, we used a desktop device (SkyScan 1272, Bruker microCT, Kontich, Belgium) with the following settings: tube voltage 40 kV, tube current 250 μA, isotropic voxel size 2.0 μm, exposure time 1815 ms, image resolution 4032x2688, no additional filtering, number of projections 2400 and averaging 5 frames/projection. NRecon software (Bruker microCT, V 1.6.20.4) was used for image reconstruction from acquired projections. During image reconstruction, beam-hardening and ring-artifact corrections were applied[21].

Local orientation analysis

Local orientation analysis provides the local spatial 3D orientation of tissue structures. Orientation analysis was conducted with CTAn software (Bruker microCT, Local Orientation plugin, ver. 1.18) which calculates the local fiber orientation using the method of Straumit et al. (2015) to determine the principal direction of voxels using structure tensors in μCT image data (Fig. 1)[24]. The analysis calculates theta (Θ) angles (polar angles) for each voxel from the structure tensors to define the orientation direction of the object within the integration window.

First, a cubic 1800 μm x 1800 μm x 1800 μm sized volume-of-interest (VOI) from the middle of the meniscus posterior horn piece was selected from the reconstructed 3D μCT image stack for the local orientation analysis (Fig. 2). The selected VOI dimensions were chosen due to computational limitations and to include mostly the collagen fiber bundles in the middle layer and not in the superficial or lamellar layers, while avoiding imaging artifacts and largest calcifications that do not account for the orientation information.

Local orientation analysis was applied to the selected VOIs from all the samples with an integration window with a size of 19 voxels, *i.e.*, the diameter that is used to calculate the direction gradient for orientation angle. In the beginning of the analysis, the μCT images are converted into 3D arrays of grey scale values from which structure tensors can be defined as shown in Fig. 1. The smallest eigenvalue and the corresponding eigenvector from decomposition of the structure tensor matrix give the direction of the local fiber orientation (polar angle Θ) for the voxel. The procedure filters falsely classified voxels by comparing alignments of neighboring voxels in the integration window[24]. The polar angle Θ is in the Z dimension perpendicular to the cross-section X-Y image plane. Polar angle $\Theta = 0$ is at 90 degrees to the X-Y plane to Z dimension. Figure 2D shows how the polar angle Θ is defined between 0 and 90 degrees.

A global background thresholding and subtraction were implemented on the VOIs after local orientation analysis to prioritize calculating orientations from intact collagen fibers over loose connective tissue. Finally, the percentage of voxels at each angle (0-90 degrees) in each sample was calculated. Lower orientation angles indicate more disorganization or non-normal orientations for the collagen fibers. In contrast, higher orientation angles present the dominating circumferential orientation in the middle layer of intact menisci.

Statistical analyses

We present the data as the percentage of voxel per given angle (0 to 90 degrees) for each sample in the figures. Further, we calculated the mean angle in each sample as a weighted average to account for the different number of voxels in each sample. We estimated unadjusted differences and also differences adjusted for age and BMI. We did not consider adjustment for sex, as the number of males and females was the same in OA and donors. To analyze the differences in mean angle between the groups, we used a linear regression model weighted by the total number of voxels in each sample with clustered standard errors to account for the dependence of samples coming from the same individual[25]. The group with 4 levels (medial OA, lateral OA, medial donor, lateral donor) was included as independent variable, with medial OA being the reference category. Further, to analyze the shape of the distribution of voxels across angles, we used Poisson regression model. The outcome was the percentage of voxels at a given angle. The independent variables included restricted cubic splines with knots at 5^{th}, 10^{th}, 30^{th}, 80^{th} and 90^{th} percentile of angles, group (OA vs donor) and interaction between group and the restricted cubic splines to allow for different shape of the relationship in each group. Further, to account for dependence of the observations coming from the same person we included a random intercept for individual. We fitted a separate model for medial compartment and a separate model for the lateral compartment. In a sensitivity analysis, we additionally adjusted for age and body mass index (BMI). The observed and fitted data can be seen in the supplementary material (Fig. S1). From these models, we extracted predicted group specific means with 95% CIs to illustrate the group specific trajectories with uncertainty at all angles.

Results

Descriptive statistics on the study participants, both OA patients and deceased donors in Table 1. The mean age of OA patients was higher than the mean age of donors while mean height and mean weight were similar between the two groups.

Collagen fiber bundles in HMDS-treated meniscal samples were successfully depicted in 3D using μCT. In medial donor, lateral donor and lateral OA samples, meniscus bundles were aligned circumferentially around the inner border of meniscus. In the medial OA meniscus, the organized structure of collagen network was lost, and the main orientation was shifted away from the circumferential alignment. In Figure 3, we show example images of μCT 3D volumes from OA patients and deceased donors, their selected VOIs and finally analyzed VOIs representing orientation angles of the meniscus microstructure. Furthermore, all selected and analysed 3D μCT volumes are presented in the supplementary material (Figures S3–S6)

In quantitative local orientation analysis and statistical comparison between the medial OA group and other sample groups, we observed 24° (95% CI 18, 31), 25° (95% CI 15, 34) and 25° (95% CI 16, 35) lower orientation angles in medial OA menisci compared to medial donor, lateral OA, and lateral donor menisci respectively (Table 2). Furthermore, medial donor, lateral OA and lateral donor menisci yielded similar mean angles with 68°, 66° and 68°, respectively. The orientation angles between lateral OA and lateral donor menisci were also similar with a mean difference of 2°.

In Figure 4, we present the percentage of voxels as a function of orientation angle in the sample groups, showing diverse distribution in medial OA menisci with increase in low orientation angles and decrease in high orientation angles compared to other groups. Medial donor and lateral OA menisci had similar low and high angle distributions, while medial donors had slightly higher amount of low angle orientations of collagen fibers (Fig. 4). Lateral donor menisci had the smallest amount of low angle orientations indicating the most intact (normal) tissue. In Figure 5A we show the percentage of voxels as a function of orientation angle in each sample from OA samples and in Figure 5B from donor samples. The results after adjustment for age and BMI were essentially the same (Table S2).

Discussion

We found that using our HMDS-based sample drying protocol together with μCT imaging, it is possible not only to visualize, but also to quantitatively analyze the local microstructural organization of collagen network in the posterior horn of human meniscus in 3D. The results of the local microstructural orientation analysis indicate substantial differences in collagen organization between osteoarthritic and donor medial posterior horn menisci. Increased disorganization of collagen fiber structure in the medial OA samples suggest a strong association between meniscus collagen (dis)organization and knee OA, where the orientation of fibers in the menisci from OA knees was on average 15 to 30 degrees lower compared to other groups.

We found increased tissue disorganization in the medial OA menisci, quantitatively indicated by a large difference in local orientation angles of collagen fiber bundles in the medial OA menisci when compared to lateral donor, lateral OA and medial donor menisci (Table 2, Fig. 4). Similarly, the estimated mean orientation angle in medial OA menisci was lower compared to all other groups (Table 2). In a related mass spectrometry study using meniscus tissue plugs from same OA patients and donors as in our study, several matrix proteins such as matrix metalloproteinase 3 and TIMP1 were found in higher intensities in the medial OA menisci compared to medial reference menisci[26]. These results could be indicative of changes in the ECM, which, in our study are shown as collagen matrix disorganization. Furthermore, our results are supported by a previous study using transmission electron microscopy, where osteoarthritic meniscus tissue was reported to have degenerated ECM and disorganized collagen fiber network when compared to healthy tissue[19]. The disorganization is suggested to be caused by meniscal hypertrophy[20]. This affects a large proportion of people with end-stage knee OA who experience edematous swelling of the tissue, especially in the medial meniscus, which could be related to meniscal extrusion, *i.e.* unloading of the tissue frequently seen in end-stage medial compartment knee OA[20,27,28]. Moreover, degeneration of meniscus is reported to increase the biosynthesis of water-binding proteoglycans that, in turn, may increase osmotic pressure and swelling[8,19,20]. Furthermore, hypertrophy in meniscus due to increased proteoglycan content is closely related to increased disorganization of collagenous structure and decreased collagen content[8,19,20]. Recent studies have reported that circumferential collagen bundles in radial cross-section are organized as polygons in a honeycomb-like shape with a diameter of 0.6-1mm[29,30]. Each polygon includes smaller compartments with circular pores inside them and gaps between each polygon to allow fluid flow through the meniscus[30]. The disruption

in collagen structure could, therefore, be caused by the swelling of these fluid compartments, which causes the collagen bundles to burst from within, as seen in our μCT images of osteoarthritic samples. This hypertrophy-induced swelling of meniscus is further supported by our previous study, in which we found that intact menisci were smaller in size than degenerated menisci[21]. Consequently, we believe that in OA hypertrophy has a great impact on the disruption of large proportion of the collagen network in meniscus. However, these effects and their association with commonly observed meniscal tears and extrusion require further study.

From our quantitative μCT analyses, we observed several similarities in the microstructural local orientations between medial donor, lateral OA, and lateral donor meniscus. Additionally, the estimated mean orientation angles of medial donor, lateral OA and lateral donor were similar (68°, 66° and 68°, respectively). In our previous study, we reported similar histopathological scores for the same sample set between lateral donor, medial donor and lateral OA groups of meniscus posterior horn[21]. In the present study, out of these three groups, lateral donor meniscus had the lowest amount of small angle orientations suggesting higher preservation of its microstructural organization than in medial donor and lateral OA meniscus. Moreover, in Figure 4, slight differences in the angle distribution between the lateral OA and the lateral donor menisci can be observed. In the lateral meniscus with medial side OA one could expect minor organizational changes compared to the lateral donor, even when their Outerbridge grades were 0 or I. However, judging from the confidence intervals, differences between donors and OA in the lateral compartment, if any, are expected to be smaller than in the medial compartment. Furthermore, the medial donor meniscus had slightly more degenerated and disorganized collagen network compared to the lateral donor meniscus. This could be expected since the weight-bearing function and biomechanical workload on the medial side of meniscus is often higher compared to the lateral side[31,32]. It is also possible that the donor menisci have some “pre-osteoarthritic” changes which would occur most likely in the medial side. Furthermore, between medial donor and lateral OA meniscus, medial donor meniscus had higher amount of small angle orientations indicating higher disorganization in its microstructure. Thus, our results suggest that the disorganization of collagen network in meniscus is more prevalent in the medial donor meniscus than in the lateral meniscus with end-stage medial compartment knee OA. In addition, this medial meniscus susceptibility to degeneration is supported by previous study showing that the medial meniscus is more vulnerable to meniscal tears and degeneration than lateral meniscus[33].

Previously established methods for the characterization of collagen orientation in AC and meniscus include two-dimensional polarized light microscopy (PLM)[12,34,35], 3D advanced microscopy such as multiphoton microscopy and second-harmonic generation microscopy[16,29,30] and small angle x-ray diffraction techniques[36]. However, all of these techniques are limited to 5 to 60 μm thin tissue sections, losing the real 3D information because a single collagen fiber averages between 5-10 μm in diameter and collagen fiber bundles together are even larger[11,13]. We have reported that our HMDS-based μCT method enables the measurement of larger volumetric structures in human posterior horn meniscus than conventional 2D section-based histology or above-mentioned methods. Furthermore, in the beginning of degeneration the meniscal surface may remain intact while distinct changes

in meniscal internal structure and composition are already observed[20]. For further studies, with this method it is possible to measure quantitatively the collagen fiber bundle orientations from any compartment or layer of meniscus to study the increasing disorganization of collagen network in OA.

In principle, it is possible to compare our collagen network disorganization results in meniscus with the disorganization of collagen network in AC. In fact, our HMDS protocol has been applied to quantitatively determine the orientation of ECM in AC[23]. However, while meniscus and AC share similarities in their structural layers, the collagen network is completely different in the circumferentially organized middle layer of meniscus compared to the deep layer of AC[4,11,37,38]. Thus, in both meniscus and AC, the disorganization of collagen network has similar features and can be quantitatively measured with our method and compared to each other with this limitation considered.

Different methods to characterize the structural orientations have been developed for different materials and tissues. Instead of structure tensors, it is possible to prepare an application of an anisotropic filter and perform a step by step rotation of a region in the image to find the most probable orientation of fibers[39] or do counting of intersections in μCT-images with fiber-matrix boundary based on the Mean Intercept Length concept[40]. In medical research, diffusion tensor image analysis is widely used in magnetic resonance imaging (MRI) to characterize microstructural changes by measuring orientations from diffusing water molecules in brain tissue[41]. In our study, we used HMDS-based protocol, which dries the sample to enable μCT imaging with high resolution. Local orientation analysis was tested to be compatible with HMDS-based dried meniscus samples and μCT imaging. It has also been reported for having low uncertainty when classifying voxels[24].

The present study has some important limitations. First, the menisci specimens were frozen after collection and then thawed before the initiation of the study. In a previous study, it was reported that freezing may cause changes in the meniscus collagen network, including shrinking in collagen fiber diameters and higher disorder in their alignment[42]. However, we performed the same preparation protocol to all samples, both from OA cases and donors, and therefore, the results are more likely to be comparable. Second, HMDS-based sample drying method preserves the sample to enable the μCT imaging but may not truly reflect the sample as it was *in vivo*. Furthermore, the increase of water content and the decrease of collagen content in the degenerated meniscus compared to donor meniscus introduces a different ratio of constituents between OA and donor meniscus[8,20]. Thus, it is theoretically possible that HMDS-based drying would cause larger shrinking of OA samples compared to donor samples. However, this difference should be minimal in practice as the HMDS reagent is believed to cross-link proteins (collagen) and it has lower surface tension compared to water[43]. This should prevent the tissue from collapsing in all cases. Moreover, even if the shrinkage due to evaporation of water is minimal, it may be a possible limitation of this contrast method due to having a greater effect in the degenerated meniscus with higher water content[8]. Third, some bony attachment of the posterior root may to various extent be left in the meniscus samples after the extraction. However, our VOI is from the posterior horn distant to the ligamentous attachment and, thus, the meniscal root is not included in the analyses. Fourth, μCT-imaging technique may introduce ring artifacts, which induce error to

the orientation angle values in affected voxels. Fifth, we acknowledge that the Poisson regression and splines models work best with larger sample sizes but, considering that the splines are based on a large number of voxels, we find our modeling approach reasonable considering the exploratory nature of the study. As a final limitation, we grouped male and female specimen together due to otherwise limited sample numbers, but the number of males and females was the same in both OA and donors.

To conclude, the local orientation analysis from HMDS-treated samples imaged with conventional desktop μCT allows visualization and quantitative measurements of the collagen fiber network in 3D in the human meniscus posterior horn. We conclude a higher disorganization of the collagen network in medial OA menisci when compared to lateral donor, medial donor and lateral OA menisci.

Supplementary Material

Refer to Web version on PubMed Central for supplementary material.

Acknowledgements

This project has received funding from the European Research Council (ERC) under the European Union's Horizon 2020 research and innovation programme (grant agreement No 771121) and under the European Union's Seventh Framework Programme (FP/2007-2013) (grant agreement No 336267). This work was also supported by the Swedish Research Council (Dnr 2014-2348), the Foundation for Research in Rheumatology (FOREUM) (018EnglundPreCl), the Greta and Johan Kock Foundation, the Swedish Rheumatism Association, the Österlund Foundation, the Governmental Funding of Clinical Research program within the National Health Service (ALF) in Sweden, and the Faculty of Medicine, Lund University, Sweden.

We would like to thank the staff of Tissue Donor Bank at Skåne University Hospital, the Department of Forensic Medicine in Lund, and the MENIX clinical personnel at Trelleborg Hospital for collaborating with the sample collection.

Role of the funding source

The funders had no role in study design, data collection and analysis, decision to publish, or preparation of the manuscript.

References

1. Makris EA, Hadidi P, Athanasiou KA. The knee meniscus: Structure-function, pathophysiology, current repair techniques, and prospects for regeneration. Biomaterials. 2011; 32(30):7411–7431. DOI: 10.1016/j.biomaterials.2011.06.037 [PubMed: 21764438]
2. Kelly, MA, Fithian, DC, Chern, KY, Mow, VC. Structure and Function of the Meniscus: Basic and Clinical ImplicationsBiomechanics of Diarthrodial Joints. Springer; New York: 1990. 191–211.
3. Fithian DC, Kelly MA, Mow VC. Material properties and structure-function relationships in the menisci. Clinical Orthopaedics and Related Research. 1990; :19–31. DOI: 10.1097/00003086-199003000-00004
4. McDevitt CA, Webber RJ. The ultrastructure and biochemistry of meniscal cartilage. Clinical Orthopaedics and Related Research. 1990; :8–18. DOI: 10.1097/00003086-199003000-00003
5. Walker PS, Erkman MJ. The role of the menisci in force transmission across the knee. Clin Orthop Relat Res. 1975; 109:184–192. DOI: 10.1097/00003086-197506000-00027
6. Messner K, Gao J. The menisci of the knee joint. Anatomical and functional characteristics, and a rationale for clinical treatment. J Anat. 1998; 193(2):161–178. DOI: 10.1046/j.1469-7580.1998.19320161.x [PubMed: 9827632]

7. Rath E, Richmond JC. The menisci: Basic science and advances in treatment. Br J Sports Med. 2000; 34(4):252–257. DOI: 10.1136/bjsm.34.4.252 [PubMed: 10953895]
8. Herwig J, Egner E, Buddecke E. Chemical changes of human knee joint menisci in various stages of degeneration. Ann Rheum Dis. 1984; 43(4):635–640. DOI: 10.1136/ard.43.4.635 [PubMed: 6548109]
9. Mow, V, Huiskes, R. Basic Orthopaedic Biomechanics & Mechano-Biology. 3rd. Mow, VC, H, R, editors. Lippincott Williams & Wilkins; 2005.
10. Fox AJS, Bedi A, Rodeo SA. The Basic Science of Human Knee Menisci: Structure, Composition, and Function. Sports Health. 2012; 4(4):340–351. DOI: 10.1177/1941738111429419 [PubMed: 23016106]
11. Petersen W, Tillmann B. Collagenous fibril texture of the human knee joint menisci. Anat Embryol (Berl). 1998; 197(4):317–324. DOI: 10.1007/s004290050141 [PubMed: 9565324]
12. Aspden RM, Yarker YE, Hukins DW. Collagen orientations in the meniscus of the knee joint. J Anat. 1985; 140(Pt 3):371–380.Accessed January 21, 2020 [PubMed: 4066476]
13. Rattner JB, Matyas JR, Barclay L, Holowaychuk S, Sciore P, Shrive NG, et al. New understanding of the complex structure of knee menisci: Implications for injury risk and repair potential for athletes. Scand J Med Sci Sports. 2011; 21(4):543–553. DOI: 10.1111/j.1600-0838.2009.01073.x [PubMed: 20459477]
14. Campo-Ruiz V, Patel D, Anderson RR, Delgado-Baeza E, González S. Evaluation of human knee meniscus biopsies with near-infrared, reflectance confocal microscopy. A pilot study. Int J Exp Pathol. 2005; 86(5):297–307. DOI: 10.1111/j.0959-9673.2005.00439.x [PubMed: 16191102]
15. Andrews SHJ, Rattner JB, Abusara Z, Adesida A, Shrive NG, Ronsky JL. Tie-fibre structure and organization in the knee menisci. J Anat. 2014; 224(5):531–537. DOI: 10.1111/joa.12170 [PubMed: 24617800]
16. Brown CP, Houle M-A, Popov K, Nicklaus M, Couture C-A, Laliberté M, et al. Imaging and modeling collagen architecture from the nano to micro scale. Biomed Opt Express. 2014; 5(1):233. doi: 10.1364/boe.5.000233
17. Fisher MB, Henning EA, Söegaard N, Bostrom M, Esterhai JL, Mauck RL. Engineering meniscus structure and function via multi-layered mesenchymal stem cell-seeded nanofibrous scaffolds. J Biomech. 2015; 48(8):1412–1419. DOI: 10.1016/j.jbiomech.2015.02.036 [PubMed: 25817333]
18. Englund M, Guermazi A, Lohmander SL. The Role of the Meniscus in Knee Osteoarthritis: a Cause or Consequence? Radiol Clin North Am. 2009; 47(4):703–712. DOI: 10.1016/j.rcl.2009.03.003 [PubMed: 19631077]
19. Battistelli M, Favero M, Burini D, Trisolino G, Dallari D, De Franceschi L, et al. Morphological and ultrastructural analysis of normal, injured and osteoarthritic human knee menisci. Eur J Histochem. 2019; 63(1) doi: 10.4081/ejh.2019.2998
20. Pauli C, Grogan SP, Patil S, Otsuki S, Hasegawa A, Koziol J, et al. Macroscopic And Histopathologic Analysis Of Human Knee Menisci In Aging And Osteoarthritis. Osteoarthr Cartil. 2011; 19(9):1132–1141. DOI: 10.1016/j.joca.2011.05.008
21. Kestilä I, Folkesson E, Finnilä MA, Turkiewicz A, Önnerfjord P, Hughes V, et al. Three-dimensional microstructure of human meniscus posterior horn in health and osteoarthritis. Osteoarthr Cartil. 2019; 27(12):1790–1799. DOI: 10.1016/j.joca.2019.07.003
22. Kestilä I, Thevenot J, Finnilä MA, Karhula SS, Hadjab I, Kauppinen S, et al. In vitro method for 3D morphometry of human articular cartilage chondrons based on micro-computed tomography. Osteoarthr Cartil. 2018; 26(8):1118–1126. DOI: 10.1016/j.joca.2018.05.012
23. Rieppo L, Karhula S, Thevenot J, Hadjab I, Quenneville E, Garon M, et al. Determination of Extracellular Matrix Orientation of Articular Cartilage in 3D Using Micro-Computed Tomography. Osteoarthr Cartil. 2017; 25 S254 doi: 10.1016/j.joca.2017.02.428
24. Straumit I, Lomov SV, Wevers M. Quantification of the internal structure and automatic generation of voxel models of textile composites from X-ray computed tomography data. Compos Part A Appl Sci Manuf. 2015; 69:150–158. DOI: 10.1016/j.compositesa.2014.11.016
25. [Accessed November 9, 2020] Stata user manual-regress-Linear regression. http://www.stata-press.com/manuals/regress.pdf

26. Folkesson E, Turkiewicz A, Ali N, Rydén M, Hughes HV, Tjörnstrand J, et al. Proteomic comparison of osteoarthritic and reference human menisci using data-independent acquisition mass spectrometry. Osteoarthr Cartil. 2020; 0(0) doi: 10.1016/j.joca.2020.05.001
27. Jung KA, Lee SC, Hwang SH, Yang KH, Kim DH, Sohn JH, et al. High frequency of meniscal hypertrophy in persons with advanced varus knee osteoarthritis. Rheumatol Int. 2010; 30(10):1325–1333. DOI: 10.1007/s00296-009-1153-7 [PubMed: 19826824]
28. Svensson F, Felson DT, Turkiewicz A, Guermazi A, Roemer FW, Neuman P, et al. Scrutinizing the cut-off for “pathological” meniscal body extrusion on knee MRI. Eur Radiol. 2019; 29(5):2616–2623. DOI: 10.1007/s00330-018-5914-0 [PubMed: 30631922]
29. Andrews SHJ, Ronsky JL, Rattner JB, Shrive NG, Jamniczky HA. An evaluation of meniscal collagenous structure using optical projection tomography. BMC Med Imaging. 2013; 13(1):1–6. DOI: 10.1186/1471-2342-13-21 [PubMed: 23289431]
30. Vetri V, Dragnevski K, Tkaczyk M, Zingales M, Marchiori G, Lopomo NF, et al. Advanced microscopy analysis of the micro-nanoscale architecture of human menisci. Sci Rep. 2019; 9(1) doi: 10.1038/s41598-019-55243-2
31. Morrison JB. The mechanics of the knee joint in relation to normal walking. J Biomech. 1970; 3(1):51–61. DOI: 10.1016/0021-9290(70)90050-3 [PubMed: 5521530]
32. Andriacchi TP. Dynamics of knee malalignment. Orthop Clin North Am. 1994; 25(3):395–403.Accessed October 21, 2020 [PubMed: 8028883]
33. Englund M, Roos EM, Lohmander LS. Impact of type of meniscal tear on radiographic and symptomatic knee osteoarthritis: A sixteen-year followup of meniscectomy with matched controls. Arthritis Rheum. 2003; 48(8):2178–2187. DOI: 10.1002/art.11088 [PubMed: 12905471]
34. Danso EK, Oinas JMT, Saarakkala S, Mikkonen S, Töyräs J, Korhonen RK. Structure-function relationships of human meniscus. J Mech Behav Biomed Mater. 2017; 67:51–60. DOI: 10.1016/j.jmbbm.2016.12.002 [PubMed: 27987426]
35. Király K, Hyttinen MM, Lapveteläinen T, Elo M, Kiviranta I, Dobai J, et al. Specimen preparation and quantification of collagen birefringence in unstained sections of articular cartilage using image analysis and polarizing light microscopy. Histochem J. 1997; 29(4):317–327. DOI: 10.1023/A:1020802631968 [PubMed: 9184847]
36. Moger CJ, Barrett R, Bleuet P, Bradley DA, Ellis RE, Green EM, et al. Regional variations of collagen orientation in normal and diseased articular cartilage and subchondral bone determined using small angle X-ray scattering (SAXS). Osteoarthr Cartil. 2007; 15(6):682–687. DOI: 10.1016/j.joca.2006.12.006
37. Ulrich-Vinther M, Maloney MD, Schwarz EM, Rosier R, O’Keefe RJ. Articular cartilage biology. J Am Acad Orthop Surg. 2003; 11(6):421–430. DOI: 10.5435/00124635-200311000-00006 [PubMed: 14686827]
38. Carballo CB, Nakagawa Y, Sekiya I, Rodeo SA. Basic Science of Articular Cartilage. Clin Sports Med. 2017; 36(3):413–425. DOI: 10.1016/j.csm.2017.02.001 [PubMed: 28577703]
39. Dietrich S, Gebert JM, Stasiuk G, Wanner A, Weidenmann KA, Deutschmann O, et al. Microstructure characterization of CVI-densified carbon/carbon composites with various fiber distributions. Compos Sci Technol. 2012; 72(15):1892–1900. DOI: 10.1016/j.compscitech.2012.08.009
40. Bernasconi A, Cosmi F, Hine PJ. Analysis of fibre orientation distribution in short fibre reinforced polymers: A comparison between optical and tomographic methods. Compos Sci Technol. 2012; 72(16):2002–2008. DOI: 10.1016/j.compscitech.2012.08.018
41. Westin CF, Maier SE, Mamata H, Nabavi A, Jolesz FA, Kikinis R. Processing and visualization for diffusion tensor MRI. Med Image Anal. 2002; 6(2):93–108. DOI: 10.1016/S1361-8415(02)00053-1 [PubMed: 12044998]
42. Gelber PE, Gonzalez G, Lloreta JL, Reina F, Caceres E, Monllau JC. Freezing causes changes in the meniscus collagen net: A new ultrastructural meniscus disarray scale. Knee Surgery, Sport Traumatol Arthrosc. 2008; 16(4):353–359. DOI: 10.1007/s00167-007-0457-y
43. Nation JL. A new method using hexamethyldisilazane for preparation of soft insect tissues for scanning electron microscopy. Biotech Histochem. 1983; 58(6):347–351. DOI: 10.3109/10520298309066811

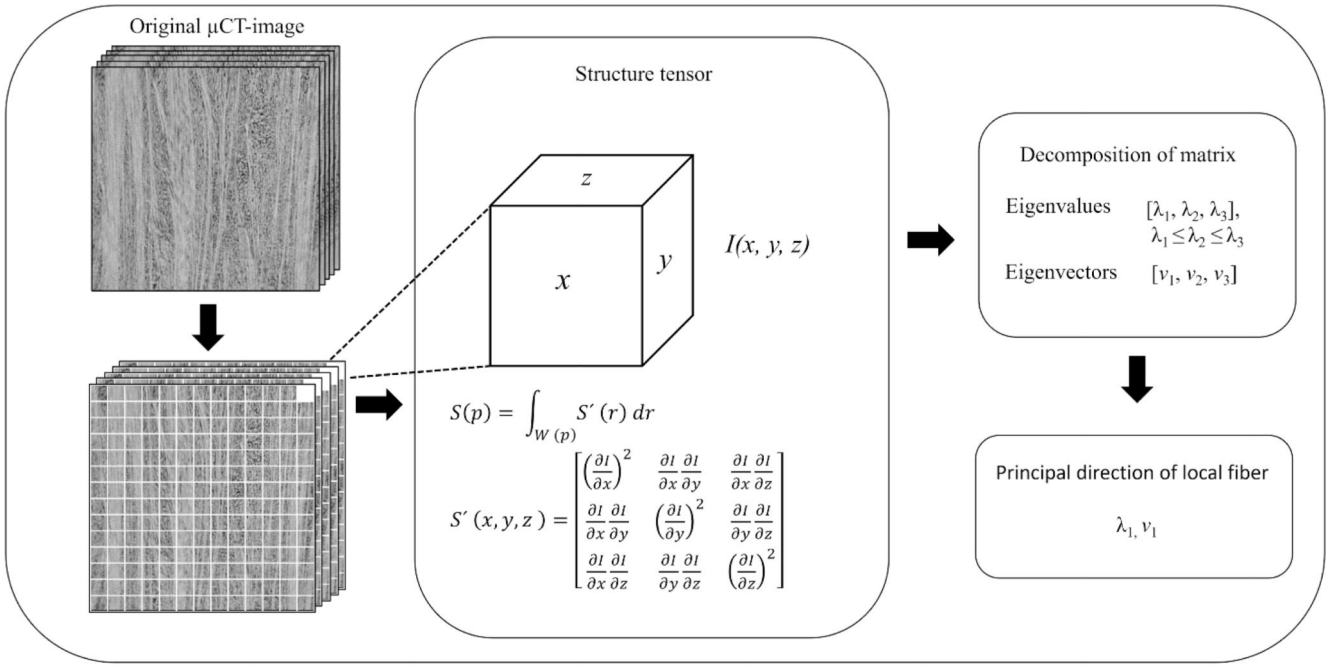

Figure 1.

Schematic representation of 3D local orientation analysis. The principal orientation direction is calculated from the image by storing the original µCT images as 3D arrays of grey values using structure tensors. Eigenvalue decomposition of this structure tensor matrix, three eigenvalues and corresponding eigenvectors are produced. The smallest eigenvalue represents the principal direction of local fiber orientation. In the equation, $W(p)$ is the integration window, vector p is position of integration window, and vector r with the components (x, y, z) is the single point in image I relative to the integration window[24]. More details can be found in in ref[24].

Europe PMC Funders Author Manuscripts

Europe PMC Funders Author Manuscripts

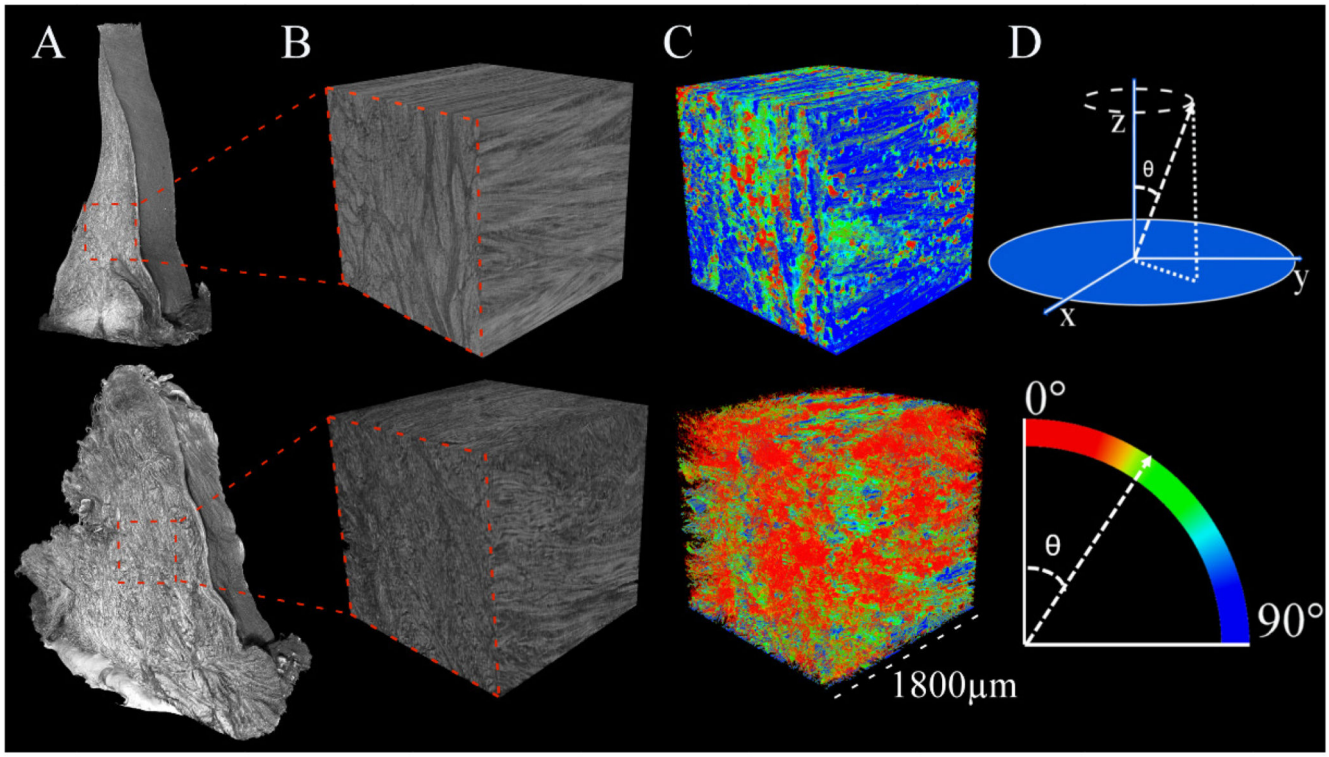

Figure 2.

A) Representative µCT 3D reconstructions of tissue pieces acquired from posterior horns of meniscus from a healthy donor on the top row and a total knee replacement (TKR) patient on the bottom row. B) A cubic volume-of-interest (VOI) was selected from the middle of the meniscus piece for local orientation analysis. C) VOIs with calculated orientations show mean angles for each voxel with dominantly high angles in the donor sample and dominantly low angles in the TKR sample. D) Graphical illustration how polar angle theta (∢) is calculated in the 3D space. Color bar shows the representative mean orientation angle in each voxel.

Europe PMC Funders Author Manuscripts

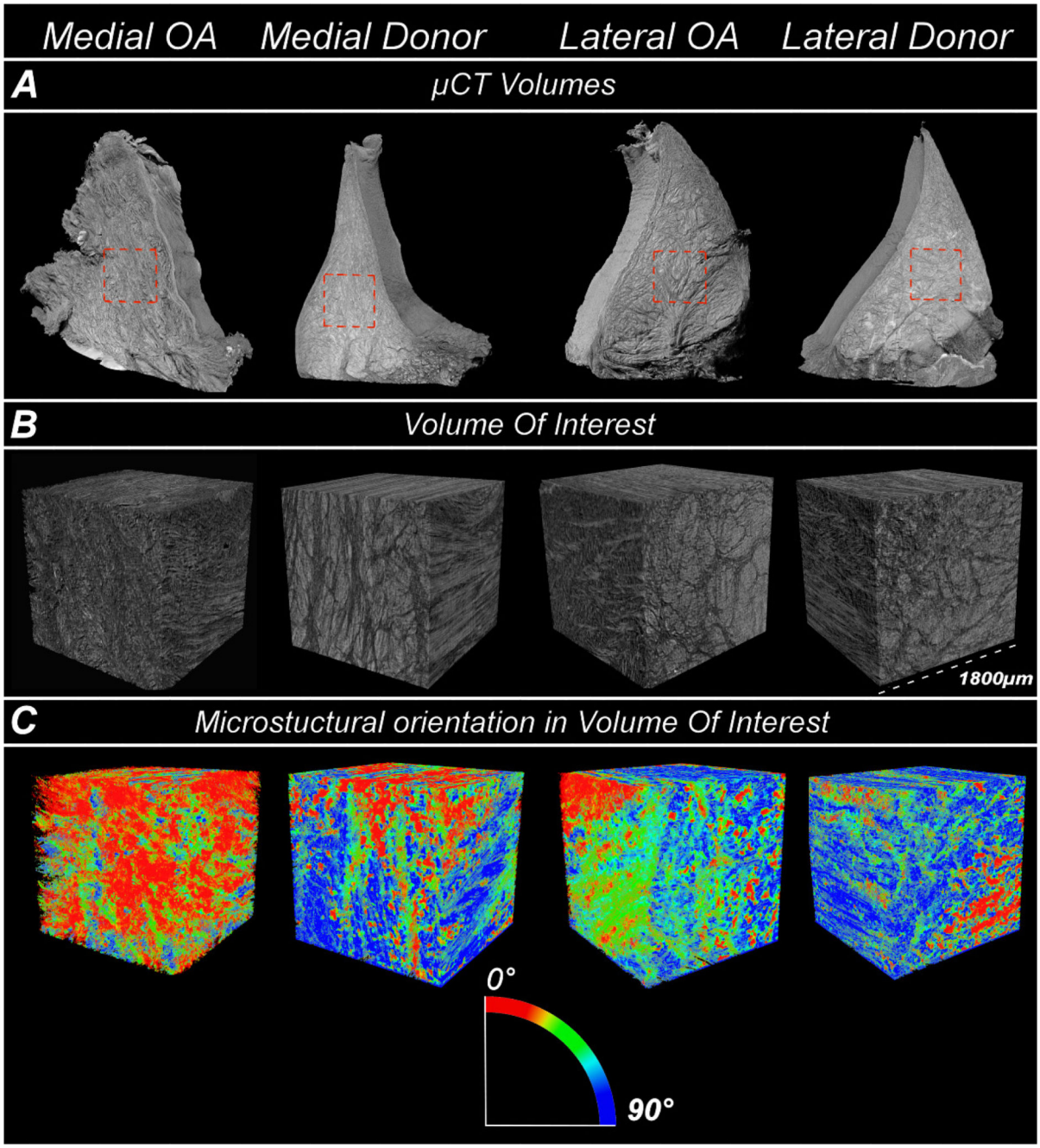

Figure 3.

A) Representative μCT 3D volumes from medial OA, medial donor, lateral OA and lateral donor groups. B) The selected volume-of-interest (VOI) with size of 1800 μm x 1800 μm x 1800 μm from the meniscus middle layer. C) The analyzed VOIs representing orientation angles of the meniscus microstructure.

Europe PMC Funders Author Manuscripts

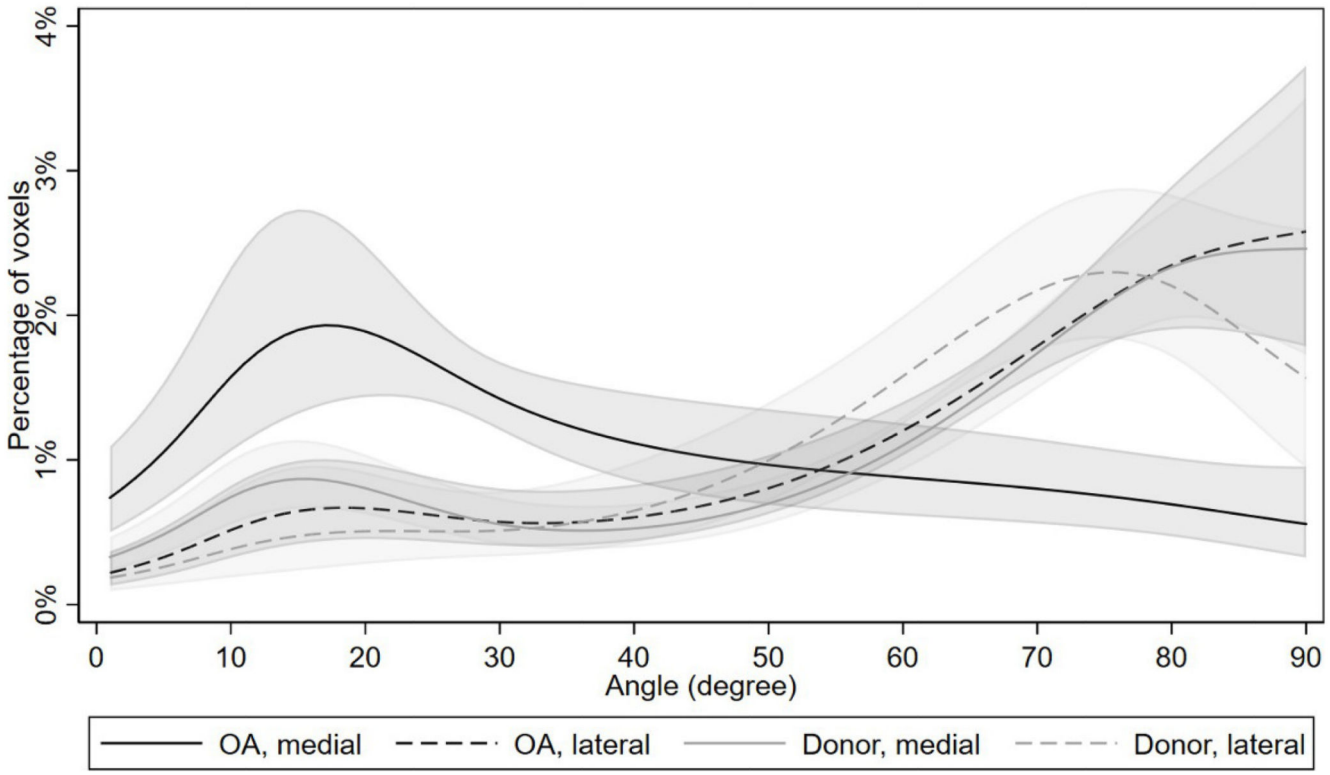

Figure 4.

The mean percentage of voxels as a function of local orientation angle (0-90 degrees) in the studied sample groups (medial OA, lateral OA, medial donor, and lateral donor) with 95% confidence intervals, as predicted from the Poisson regression model (see statistical methods section for details). Medial OA group had the highest amount of low angle orientations indicating most disorganization in the tissue when compared to all other groups. Medial donor and lateral OA groups have similar low and high angle distributions. Lateral donor group had the smallest amount of low angle orientations indicating the healthiest tissue group.

Europe PMC Funders Author Manuscripts

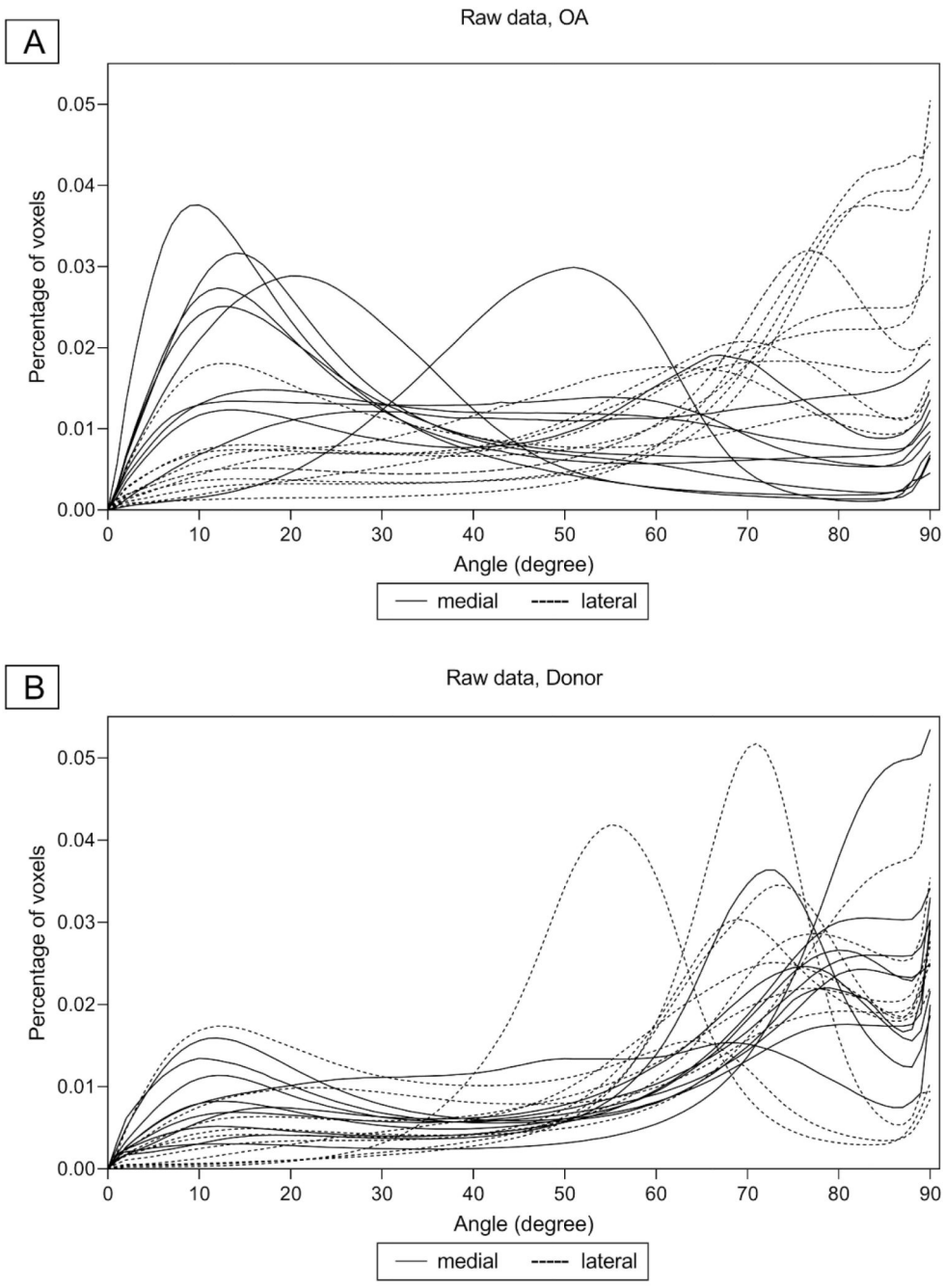

Figure 5.

The percentage of voxels at each angle for each individual sample for OA samples (A) and donor samples (B).

Europe PMC Funders Author Manuscripts

Table 1

Descriptive data on the study sample.

Group	Age	Sex	Height (cm)	Weight (kg)
	Mean (SD)	(% women)	Mean (SD)	Mean (SD)
OA patients	63 (7)	50 (50)	171 (9)	84 (13)
Donors	51 (17)	50 (50)	172 (10)	84 (27)

Europe PMC Funders Author Manuscripts

Table 2

The mean value of angles of collagen fiber bundles within the following groups: medial OA, medial donor, lateral OA and lateral donor. *Estimating the effects of age and BMI on the mean angle was not the aim of the study and are presented for transparency only.

Group	Mean	Mean estimated differences vs. medial OA (95% CI)	Mean estimated differences vs. medial OA adjusted for age and BMI (95% CI)	*Estimated effects of age and BMI for all groups
Medial OA	42			Age (per 10 years of age): 0.6 (-2.1, 3.3)
Medial donor	68	24 (18, 31)	25 (18, 32)	
Lateral OA	66	25 (15, 34)	25 (16, 36)	BMI (per 1 unit): 0.3 (-0.1, 0.7)
Lateral donor	68	25 (16, 35)	27 (16, 38)	